

Differences in thermo-mechanical properties and intermolecular charge-transfer characteristics of the aromatic polyimide PI(BPDA/PDA) from various precursors

Hsu Wen Huang^{*1}, Kazuyuki Horie^{*1}, Rikio Yokota²

¹ Department of Chemistry and Biotechnology, Graduate School of Engineering, The University of Tokyo, 7-3-1 Hongo, Bunkyo-ku, Tokyo 113-8656, Japan

² Institute of Space and Astronautical Science, 3-1-1 Yoshinodai, Sagami-hara, Kanagawa 229-0022, Japan

(Received: July 6, 1998; revised: November 9, 1998)

SUMMARY: The differences in thermo-mechanical properties and intermolecular charge-transfer (CT) characteristics of an aromatic polyimide, PI(BPDA/PDA), from polyamide acid (PAA), polyamide allyl ester (PAAE), or polyamide benzyl ester (PABE) precursors were studied. The various PI(BPDA/PDA)'s show identical uniformity in chemical structure and thermogravimetric behavior. PI(BPDA/PDA) from PAA however shows higher density and T_g and lower thermal expansion coefficient than those from PAAE and PABE, indicating the higher orderliness of the molecular packing of PI(BPDA/PDA) from PAA. Intermolecular ground-state CT complexes of PI(BPDA/PDA) from PAAE and PABE show fluorescence at longer wavelengths and wider fluorescence peak wavelength range than the one of PI(BPDA/PDA) from PAA. This suggests the wider variety of aggregation structures of PI(BPDA/PDA) from PAAE and PABE than those of PI(BPDA/PDA) from PAA. The steric hindrance of the bulky substituents of PAAE and PABE would cause an increase in the variety of aggregation structures during imidization. The shorter fluorescence lifetimes of PI(BPDA/PDA) from PAAE and PABE than the one of PI(BPDA/PDA) from PAA also confirm the differences in their intermolecular CT characteristics.

Introduction

Aromatic polyimides (PIs) have been of great interest for microelectronic applications owing to their high temperature stability, low dielectric constant, and useful mechanical properties^{1,2}. Traditionally, PIs are generally synthesized in a two-step process by the condensation reaction of a diamine and a dianhydride to form a soluble polyamide acid (PAA). The PAA precursors are then solvent cast to the desired form and thermally treated to cyclodehydrate the precursors, liberating water and forming the final PIs. Understanding the details of the imidization reaction is important to ensure optimal final properties, and critical in the design of a system involving the deposition of consecutive layers. On the other hand, an ester of the PAA, for example, the ethyl ester, can also be cyclodehydrated, producing ethanol rather than water. Such polyamide alkyl ester precursors have also been developed^{3–8}. In contrast to PAA precursors, polyamide alkyl ester precursors have improved solution properties, such as better resistance to hydrolytic degradation, lower viscosity solution with higher solid content^{3–8}, and an apparent lack of exchange reactions in solutions containing different precursors^{9–11}. Similarly, the polyamide alkyl ester precursors can also be cyclodehydrated to the identical PI by thermal treatment, as the corresponding PAA precursors, in spite of their higher imidization temperature than PAA precursors^{3,7}.

The remarkable thermal stability and other physical properties of aromatic PIs are well known to be due to the rigidity of polymer chain, and strong charge-transfer (CT) interaction between aromatic moieties (electron donor) and imide moieties (electron acceptor)^{1,2}. The origin of intermolecular CT complexes of aromatic PIs has been proved¹² and studied extensively^{13,14}. Although Fourier-transform infrared spectroscopy (FTIR) and X-ray diffraction have been used to study the degree of imidization and the approximate molecular arrangement of PIs, it is difficult to examine the aggregation structures of PIs by FTIR and X-ray diffraction. On the contrary, by using fluorescence method, it is effective to study the aggregation structures consisting of intermolecular CT complexes directly. Thus, by investigating the change in fluorescence behavior of the intermolecular CT complexes, the change in molecular aggregation structures of aromatic PIs during imidization have been studied in detail^{14,15}. According to the above studies, examining the change in CT fluorescence behavior is proved to be useful in studying the molecular aggregation structures of aromatic PIs.

The differences of a polyimide composed of biphenyl-tetracarboxylic dianhydride (BPDA) and p-phenylenediamine (PDA), PI(BPDA/PDA), prepared from different precursors, i.e., from PAA, polyamide alkyl esters^{16–18}, or photosensitive PI precursor¹⁹, have been studied by thermo-mechanical and X-ray diffraction measurements.

However, the thermo-mechanical properties and intermolecular CT characteristics of PI(BPDA/PDA) from various precursors have not been compared for elucidating the differences of their molecular aggregation structures. In the present paper, precursors with various substituents groups, i.e., a conventional PAA, a photosensitive polyamide allyl ester (PAAE), and a bulky polyamide benzyl ester (PABE), are prepared for synthesis of PI(BPDA/PDA). By using thermo-mechanical and fluorescence measurements, we study the differences in thermo-mechanical properties and intermolecular CT characteristics of PI(BPDA/PDA) from various precursors after an identical thermal imidization process.

Experimental part

Sample preparation and materials

N-Methylpyrrolidone (NMP, Tokyo Kasei) was dried with molecular sieves (4A) and vacuum distilled before use. The PAA precursor from biphenyltetracarboxylic dianhydride (BPDA) and *p*-phenylenediamine (PDA) was prepared as reported elsewhere^{12–14}. The preparation of PAAE and PABE is based on the reported work⁵) and presented in Fig. 1. After obtaining the PAA precursor, a stoichiometric amount of triethylamine as the neutralizing base and a 3-fold excess of allyl bromide (Tokyo Kasei) were added into the NMP solution of PAA, the byproduct salts were precipitated, then the solution was kept stirring for 24 h at room temperature. To precipitate and wash the PAAE precursor, 2-propanol, 1%

aqueous hydrochloric acid, and acetone were added to the solution or precipitates in the above sequence, then the PAAE was vacuum dried for 24 h at 50 °C. Similarly, by using benzyl bromide (Tokyo Kasei), the PABE precursor was prepared with the same procedure. The various precursor were dissolved in NMP again and spin-coated or bar-coated to form films, then vacuum dried for 24 h at 50 °C. The films of various precursors were then imidized at 150 °C for 1 h and at 450 °C for 1 h in vacuum to obtain PI(BPDA/PDA).

Measurements

FTIR spectra were measured with a Jasco FTIR-230S spectrophotometer.

DSC measurements were performed with a Thermal Analysis Instruments 2010 differential scanning calorimeter. Samples of about 5 mg were examined at a scanning rate of 10 °C/min under a flow of dry nitrogen.

The densities of PI films were measured by a density gradient column (carbon tetrachloride and xylene system) in a thermostat at 35 °C.

TG measurements were performed with a Thermal Analysis Instruments 2050 thermogravimetric analyzer and examined at a heating rate of 10 °C/min under nitrogen atmosphere.

TMA measurements were performed with a Rigaku TAS 200 thermo-mechanical analyzer. Samples in 14 mm × 3 mm rectangular shape with about 5–8 μm thickness were mounted between two chucks and measured at a heating rate of 10 °C/min under nitrogen atmosphere with a loaded force of 10 g. Since the thermal expansion coefficient (TEC) was

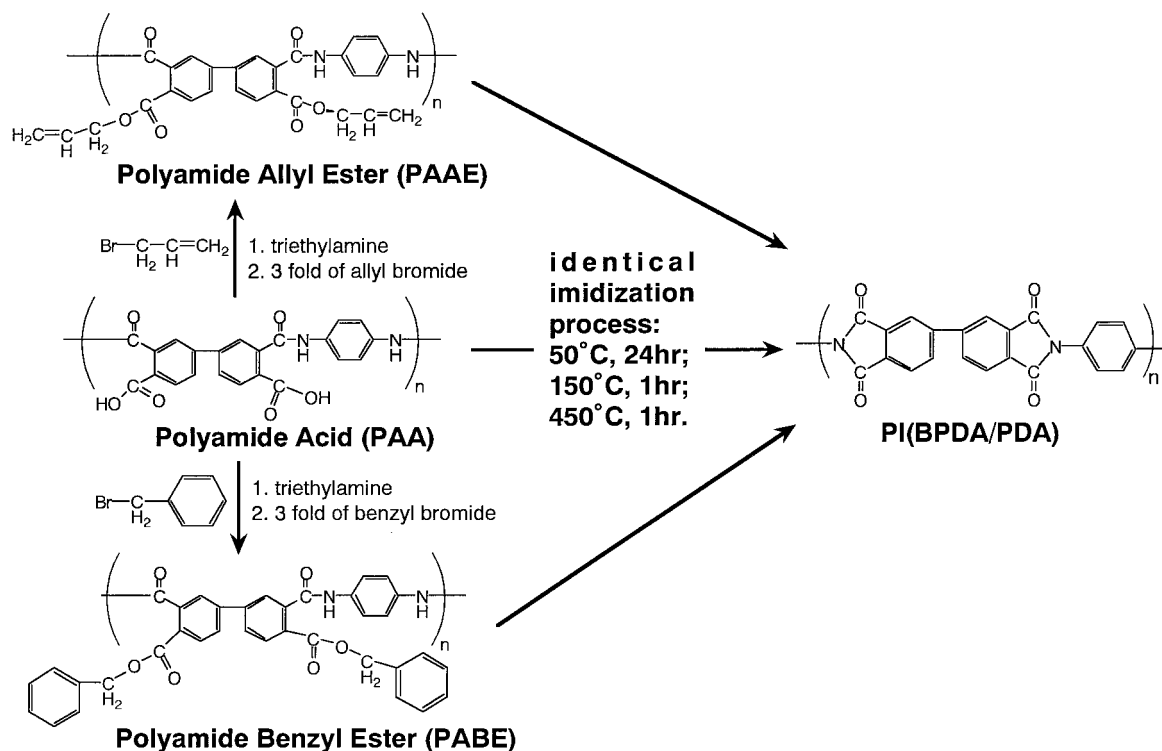


Fig. 1. Schematic diagram of preparation of PI(BPDA/PDA) from various precursors with an identical imidization process

temperature dependent, the average value between 100 and 250 °C was used as a representative value.

Fluorescence and its excitation spectra were measured with a Hitachi 850 fluorescence spectrophotometer in a front face arrangement to minimize the self-absorption.

Fluorescence lifetime measurements were performed with a Hamamatsu C4780 single-photon counting system. A nitrogen-laser-pumped dye laser (Laser Photonics Ltd., LN120C) with stilbene solution (Exciton, Inc.), emitting light centered around 420 nm, was used as an excitation pulse source. The excitation pulse was directed to the sample through an optical fiber, and the emitted light was also guided through an optical fiber to a Hamamatsu C4334 streak scope, then transformed to streak images. The delay time was controlled by a Hamamatsu C4792 trigger unit. The instrument response function of the whole system was about 1.4–1.8 ns (fwhm).

Results and discussion

Characterization of various precursors

Fig. 2 shows the FTIR spectra for the films of PAA (a), PAAE (b), and PABE (c). As can be seen in Fig. 2a, PAA shows the absorption of C=O stretching for carboxylic acid at 1714 cm⁻¹. But PAAE (b) and PABE (c) show the absorption of C=O stretching for allyl ester group and benzyl ester group at 1724 cm⁻¹ and 1721 cm⁻¹, respectively. PAAE (b) also shows two O—C—O stretching

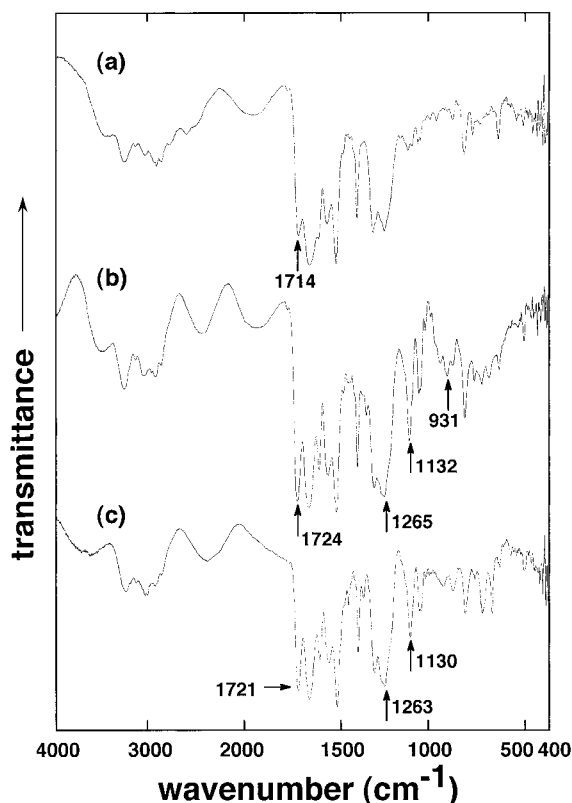


Fig. 2. FTIR spectra for the films of PAA (a), PAAE (b), and PABE (c) after vacuum drying for 24 h at 50 °C

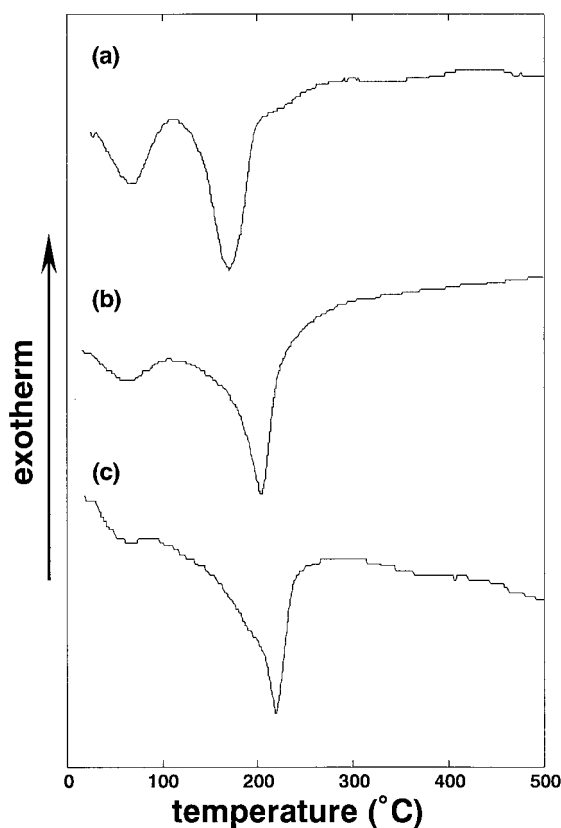


Fig. 3. DSC curves for PAA (a), PAAE (b), and PABE (c) at a heating rate of 10 °C/min

bands of allyl ester group at 1265 cm⁻¹ and 1132 cm⁻¹. Similarly, PABE (c) also exhibits two O—C—O stretching bands of benzyl ester group at 1263 cm⁻¹ and 1130 cm⁻¹. But this kind of O—C—O stretching band of ester group is not observed for PAA, which is in accord with the results of other workers^{3,5,7}. Moreover, PAAE (b) shows an allylic absorption at 931 cm⁻¹. According to the above FTIR results, esterification to a substantial extent from PAA to PAAE and PABE is confirmed.

Since it is indispensable to examine the imidization reaction temperature of various precursors for obtaining the completely imidized PI, the DSC curves of various precursors are examined, as shown in Fig. 3. For PAA (a), one can observe two endothermic peaks around 70 °C and 168 °C, which can be regarded as the water vaporization and the imidization reaction temperature, respectively. For PAAE (b), one can also observe the identical water vaporization around 70 °C, but higher imidization reaction temperature at 204 °C. Similarly, according to Fig. 3c, the imidization reaction temperature of PABE (217 °C) is also higher than that of PAA. This may be because the substituent group of esters (allyl group and benzyl group) are bulkier than the one of acid (hydrogen), and the electrophilicity of ester group is weaker than that of acid group, which is due to the higher electron density of allyl group and benzyl group in comparison with the

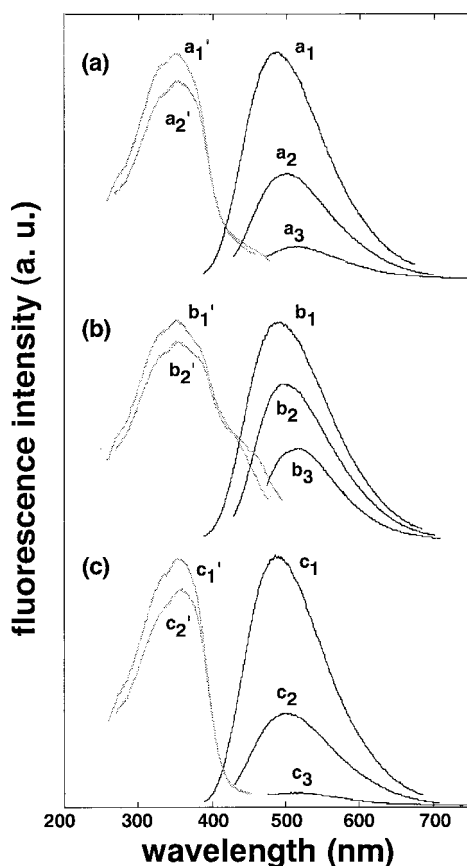


Fig. 4. Fluorescence (solid curves) and its excitation spectra (gray curves) for PAA (a), PAAE (b), and PABE (c). Fluorescence spectra with subscript 1–3 are excited at 350 nm, 400 nm, and 450 nm, respectively; fluorescence excitation spectra with subscript 1' and 2' are monitored at 490 nm and 520 nm, respectively

hydrogen^{3,7}). Based on the above DSC results, in order to obtain the same degree of the imidization for PAA, PAAE, and PABE, it is necessary to proceed the imidization process at much higher temperature than the usual imidization temperature for PAA. Thus, the imidization process was performed at 150 °C for 1 h and at 450 °C for 1 h in vacuum.

In order to compare the aggregation structures of various precursors before and after imidization, the fluorescence (solid curves) and its excitation spectra (gray curves) for PAA (a), PAAE (b), and PABE (c) were measured and depicted in Fig. 4. Independent of the substituent groups of various precursors, all the precursors show a main peak around 350 nm in fluorescence excitation spectra (a₁', b₁', c₁') and a corresponding fluorescence peak around 490 nm (a₁, b₁, c₁), which is due to the molecular interaction of excited BPDA moieties with other moieties²⁰. Moreover, by exciting at longer excitation wavelengths (400–450 nm), all the precursors show slight red shift in fluorescence peak wavelength (a₂, a₃; b₂, b₃; c₂, c₃), and their fluorescence excitation spectra monitored at 520 nm (a₂', b₂', c₂') are in accord with those monitored at

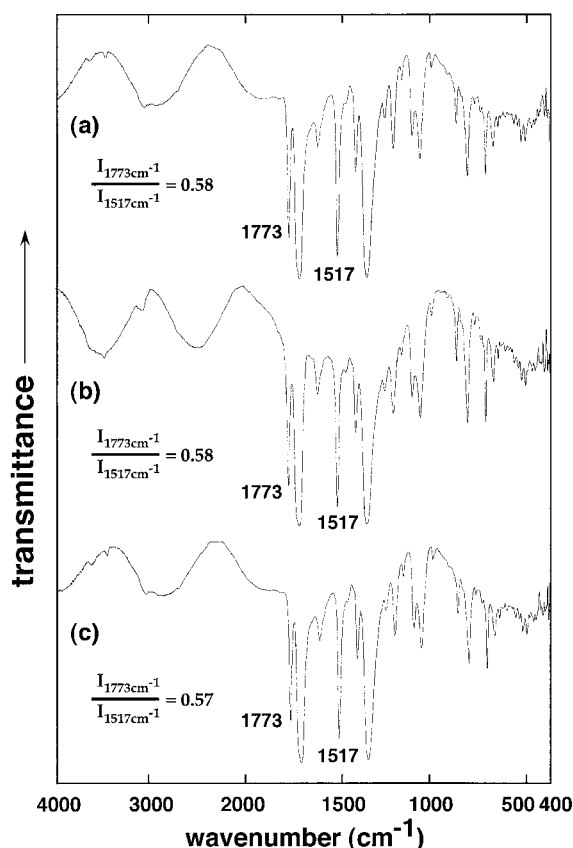


Fig. 5. FTIR spectra for PI(BPDA/PDA) films from PAA (a), PAAE (b), and PABE (c) after the identical thermal imidization process

490 nm (a₁', b₁', c₁'). This slight red shift may reflect the existence of various kinds of molecular interactions of excited BPDA moieties with other moieties in these amorphous precursors. In spite of the differences of fluorescence intensity, the fluorescence behavior of these precursors is considered to be identical. The consistency in fluorescence behavior of various precursors also suggests that these precursors are in amorphous state.

Characterization, thermal stability, and thermo-mechanical properties of PI(BPDA/PDA) from various precursors

Since it is necessary to ascertain the same degree of imidization for PI(BPDA/PDA) from various precursors, the FTIR spectra for PI(BPDA/PDA) from various precursors after the identical imidization process are presented in Fig. 5. The degree of imidization is estimated by the absorbance ratio of 1773 cm⁻¹ band (C=O stretching in imide ring) to the 1517 cm⁻¹ band (C=C stretching in benzene ring in PDA) as shown in Fig. 5. As can be seen in Fig. 5, independent of the differences of precursors, all the PI(BPDA/PDA)'s from various precursors show the same FTIR spectra and an almost identical degree of imi-

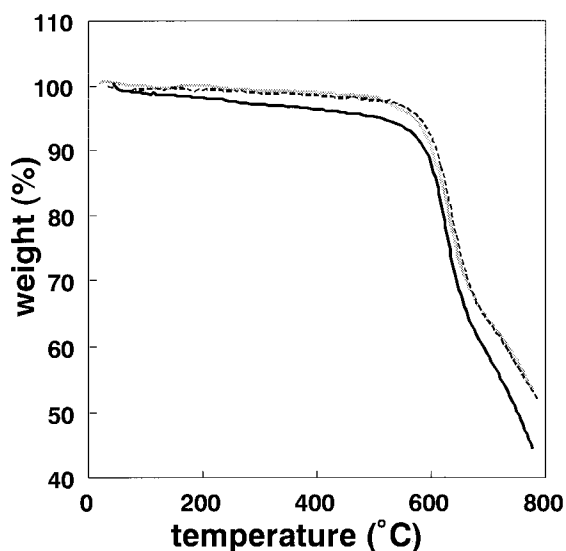


Fig. 6. TG curves of PI(BPDA/PDA) from PAA (solid curve), PAAE (dashed curve), and PABE (gray curve) after the identical imidization process

dization, which corresponds to the degree of imidization of completely imidized PI(BPDA/PDA) reported by other workers¹³). This indicates that the chemical structures and degrees of imidization of PI(BPDA/PDA) from various precursors are identical. In order to examine the uniformity in chemical structure and evaluate the thermal stability, TG curves of PI(BPDA/PDA) from various precursors after the identical imidization process are depicted in Fig. 6. Independent of the differences of precursors, all the PI(BPDA/PDA)'s from various precursors do not show any thermal degradation of byproducts, and also show identical degradation temperature at about 585–591 °C as summarized in Tab. 1. Based on the above FTIR and TG results, PI(BPDA/PDA)'s from various precursors show identical uniformity in chemical structure and the same degradation stability, and might be assumed to be identical in other physical properties. Nevertheless, the densities of these PI films shown in Tab. 1 are different from each other and the order of density is arranged as follows: PAA (1.4555 g/cm³) > PAAE (1.4480 g/cm³) > PABE (1.4463 g/cm³). This seems to imply that the

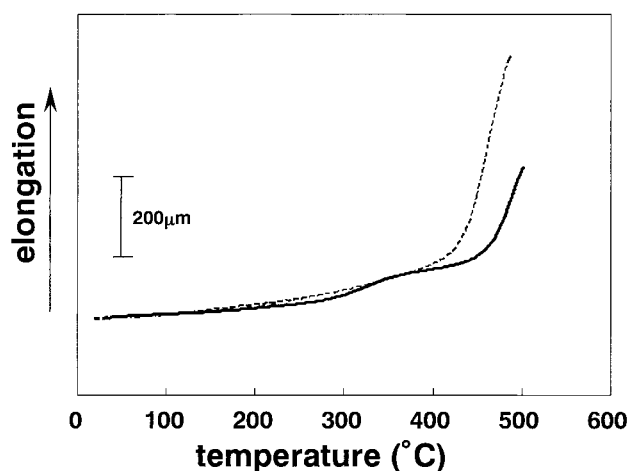


Fig. 7. TMA curves of PI(BPDA/PDA) from PAA (solid curve) and PAAE (dashed curve) after the identical imidization process

density of PI(BPDA/PDA) from polyamide esters is smaller than that from PAA, which would be due to the difference in molecular mobility during thermal cure of various precursors, caused by the differences in hydrogen-bonding ability with the solvent, imidization rate, and/or the size of the volatile group outgassed during imidization²¹).

Thermo-mechanical properties of polymers such as dimensional stability and TEC and known to be strongly related to geometry and aggregation structure in addition to chemical structure^{1,2}). Therefore, the TMA measurements were carried out to investigate the differences of density for PI(BPDA/PDA) from various precursors. Fig. 7 shows the TMA curves of PI(BPDA/PDA) from various precursors. In Fig. 7, PI(BPDA/PDA) from PAA (solid curve) reveals elongation for about 200 μm beyond T_g (455 °C). But PI(BPDA/PDA) from PAAE (dashed curve) reveals larger elongation for about 400 μm beyond T_g (423 °C). Unfortunately, the film of PI(BPDA/PDA) from PABE was too brittle and unavailable for TMA measurement, which is due to the too large substituent group to hinder the molecular packing. Moreover, according to the TEC values shown in Tab. 1, TEC of PI(BPDA/PDA) from PAA ($0.77 \times 10^{-5} \text{ K}^{-1}$) is smaller than the one from PAAE ($1.62 \times 10^{-5} \text{ K}^{-1}$). These results

Tab. 1. Thermo-mechanical and fluorescence properties of PI(BPDA/PDA) from various precursors

PI(BPDA/PDA) from various precursors	Degradation temperature ^{a)} in °C	Density in g/cm ³	T_g ^{b)} °C	TEC ^{c)} K ⁻¹	Fluorescence peak wavelength range in nm	Fluorescence lifetime (ns)	
						τ_1	τ_2
PAA	589	1.4555	455	0.77×10^{-5}	525–567	1.6	6.1
PAAE	585	1.4480	423	1.62×10^{-5}	525–600	0.8	3.3
PABE	591	1.4463	—	—	525–600	0.8	3.3

a) The onset of weight loss the TG curve.

b) The onset of elongation in the TMA curve.

c) Thermal expansion coefficient.

are in good accord with the recently reported results¹⁸⁾ for PI(BPDA/PDA) prepared from polyamide acid alkyl esters. The difference between the TEC of PI(BPDA/PDA) from PAA and that from PAAE indicates that the aggregation structures of PI(BPDA/PDA) from PAA arrange in a molecular packing with higher orderliness than those from PAAE and PABE. The interactions between the precursors and the solvent (NMP) have been suggested to lead to large differences in higher order structures of the polyimides, which in turn affect the TEC¹⁸⁾. Molecular packing of PI has been demonstrated to be deeply related to the intermolecular CT complexes^{12–15)}. Therefore, it seems effective to use fluorescence method to study the fluorescence behavior of intermolecular CT complexes for elucidating the differences of molecular packing of PI(BPDA/PDA) from various precursors.

Differences in fluorescence behavior of PI(BPDA/PDA) from various precursors

Fig. 8 shows the fluorescence (right) and its excitation spectra (left) of PI(BPDA/PDA) from various precursors. At first, we refer to the fluorescence excitation spectra for PI(BPDA/PDA) from PAA (a'_1 , a'_2 , a'_3). A main peak is observed around 350 nm, and its corresponding fluorescence peak (a_1) appears at much longer wavelength (525 nm) than the one before imidization (490 nm), which is due to the strong CT interaction between excited biphenylbisimide moieties to form the intermolecular excited-state CT complexes^{14–20)}. Moreover, related to the shoulder around 470–480 nm in the fluorescence excitation spectra, by exciting at longer excitation wavelengths (400–520 nm), another group of fluorescence peaks are observed around 538–567 nm (a_2 , a_3 , a_4), which are due to the intermolecular ground-state CT complexes at lower energy level¹⁴⁾. These intermolecular ground-state CT complexes show red-shift phenomenon by excitation at longer wavelengths (400–520 nm). This indicates the existence of various kinds of intermolecular ground-state CT complexes. But this kind of apparent red shift of fluorescence is not observed before imidization (Fig. 4a). This is because the molecular packing changes to be more ordered after imidization, and makes the moieties interact sensitively with each other to reflect the difference of molecular interaction. As to the fluorescence behavior of PI(BPDA/PDA) from PAAE (Fig. 8b), its fluorescence excitation spectra (b'_1 , b'_2 , b'_3) and fluorescence peak wavelength of intermolecular excited-state CT complex (b_1) are identical to those of PI(BPDA/PDA) from PAA. Similarly, the intermolecular excited-state CT complex of PI(BPDA/PDA) from PABE (c_1) also shows fluorescence around 525 nm. This consistency of fluorescence for the intermolecular excited-state CT complex of

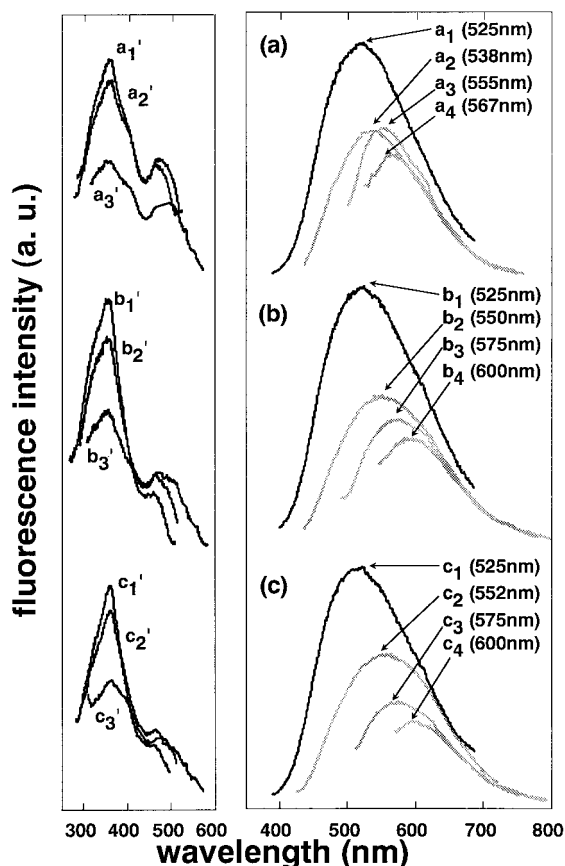


Fig. 8. Fluorescence (right) and its excitation spectra (left) for PI(BPDA/PDA) from PAA (a), PAAE (b), and PABE (c) after the identical imidization process. Fluorescence spectra with subscript 1–4 are excited at 350 nm, 400 nm, 480 nm, and 520 nm, respectively, and the values in the parenthesis are their fluorescence peak wavelengths. Fluorescence excitation spectra with subscript 1–3 are monitored at 525 nm, 550 nm, and 600 nm, respectively

PI(BPDA/PDA) from various precursors indicates the consistency of uniformity in their chemical structure, as studied by FTIR and TG measurements. However, the intermolecular ground-state complexes of PI(BPDA/PDA) from PAAE (b_2 , b_3 , b_4) show wider fluorescence peak wavelength range at 550–600 nm than those of PI(BPDA/PDA) from PAA (538–567 nm). In an analogous manner, the intermolecular ground-state complexes of PI(BPDA/PDA) from PABE (c_2 , c_3 , c_4) also show wider fluorescence peak wavelength range at 552–600 nm than those of PI(BPDA/PDA) from PAA (538–567 nm). This indicates that the structures of intermolecular ground-state CT complexes of PI(BPDA/PDA) from PAAE and PABE are in wider variety than those of PI(BPDA/PDA) from PAA. In other words, this reflects that the orderliness of molecular packing of PI(BPDA/PDA) from PAAE and PABE is lower than that of PI(BPDA/PDA) from PAA. The main aggregation structures of PI(BPDA/PDA) from PAAE and PABE strongly

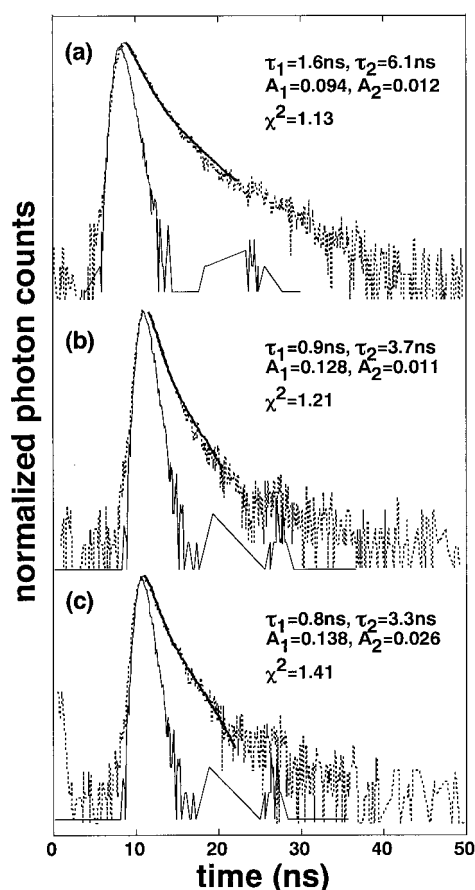


Fig. 9. Fluorescence decay profiles excited at 420 nm and monitored at 525–630 nm for PI(BPDA/PDA) from PAA (a), PAAE (b), and PABE (c) after the identical imidization process. Solid curves are excitation pulse, dotted curves are the decay profiles of the samples, and bold curves are the convoluted decay profiles

suffer from the size of bulky substituent groups which interfere with the molecular packing during imidization reaction. Additionally, the fluorescence peak wavelength of the intermolecular ground-state complex excited at 400 nm for PI(BPDA/PDA) from PAA (a_2 , $\lambda_f = 538$ nm) shows shorter fluorescence peak wavelength than those of PI(BPDA/PDA) from PAAE (b_2 , $\lambda_f = 550$ nm) or PABE (c_2 , $\lambda_f = 552$ nm). Similarly, the fluorescence peak wavelengths of other intermolecular ground-state complexes excited at longer wavelengths for PI(BPDA/PDA) from PAA (a_3 , a_4) all show shorter fluorescence peak wavelengths than those of PI(BPDA/PDA) from PAAE (b_3 , b_4) or PABE (c_3 , c_4). This may indicate that the defect aggregation structures are in a more polarized electronic state, thus emitting fluorescence at longer wavelength than those in orderly arranged aggregation structures observed in PI(BPDA/PDA) from PAA.

In order to investigate the fluorescence emission process of the intermolecular CT complexes of PI(BPDA/PDA) from various precursors, their fluorescence decay

profiles were measured and shown in Fig. 9. The fluorescence decay profile, $I_f(t)$, can be best fitted with a double exponential function:

$$I_f(t) = A_1 \times \exp(-t/\tau_1) + A_2 \times \exp(-t/\tau_2)$$

where $I_f(t)$ is the fluorescence intensity at time t , A_1 and A_2 are the pre-exponential factors, and τ_1 and τ_2 the fluorescence lifetimes. The fluorescence decay profiles for PI(BPDA/PDA) from various precursors and the results of analysis are presented in Fig. 9 and also given in Tab. 1. According to the analysis for PI(BPDA/PDA) from PAA (Fig. 9a), its fluorescence lifetimes τ_1 and τ_2 are 1.6 ns and 6.1 ns, respectively. But PI(BPDA/PDA) from PAAE (Fig. 9b) shows shorter fluorescence lifetimes, $\tau_1 = 0.8$ ns and $\tau_2 = 3.7$ ns. Similarly, PI(BPDA/PDA) from PABE (Fig. 9c) also shows shorter fluorescence lifetimes, $\tau_1 = 0.8$ ns and $\tau_2 = 3.3$ ns. These differences of fluorescence lifetimes indicate that the fluorescence emission processes of the intermolecular CT complexes of PI(BPDA/PDA) from PAA are different from those of PI(BPDA/PDA) from PAAE and PABE.

Conclusions

Intermolecular CT fluorescence behavior and thermomechanical properties of PI(BPDA/PDA) from PAA, PAAE, and PABE after an identical imidization process were compared as summarized in Tab. 1. The uniformity in chemical structure and thermogravimetry of PI(BPDA/PDA) from various precursors has been confirmed. However, according to Tab. 1, PI(BPDA/PDA) from PAA shows higher density and T_g and lower TCE than those of PI(BPDA/PDA) from PAAE and PABE. This indicates that the orderliness of molecular packing of PI(BPDA/PDA) from PAA is higher than those of PI(BPDA/PDA) from PAAE and PABE. The intermolecular ground-state CT complexes of PI(BPDA/PDA) from PAAE and PABE show fluorescence at longer wavelengths and wider fluorescence peak wavelength range than those of PI(BPDA/PDA) from PAA. This implies the formation of wider variety of aggregation structures of PI(BPDA/PDA) from PAAE and PABE than those of PI(BPDA/PDA) from PAA. The fluorescence emission processes of intermolecular CT complexes of PI(BPDA/PDA) from various precursors were also confirmed to be different from each other owing to their different fluorescence lifetimes. Study of the intermolecular CT characteristics of PI is proved to be effective in distinguishing the differences of aggregation structures among PI(BPDA/PDA) from various precursors.

Acknowledgement: H. W. H. is greatly indebted to the JSPS Research Fellowship for Young Scientists for supporting his

research and Ph.D study in the University of Tokyo. The present work is partly supported by an Grand in Aid from the Ministry of Education, Culture, and Sports of Japan (A-08405060).

- ¹⁾ "Photosensitive Polyimides: Fundamentals and Applications", K. Horie, T. Yamashita, Eds., Technomic, Lancaster 1995
- ²⁾ "Polyimides: Fundamentals and Applications", M. K. Ghosh, K. L. Mittal, Eds., Dekker, New York 1996
- ³⁾ S. Nishizaki, T. Moriwaki, *J. Chem. Soc. Jpn.* **71**, 1559 (1967)
- ⁴⁾ V. L. Bell, R. A. Jewell, *J. Polym. Sci., Part A-1* **5**, 3043 (1967)
- ⁵⁾ "Polyimides: Materials, Chemistry and Characterization", C. Feger, M. M. Khojasteh, J. E. McGrath, Eds., Elsevier, Amsterdam 1989
- ⁶⁾ N. C. Stoffel, E. J. Kramer, W. Volksen, T. P. Russell, *Polymer* **34**, 4524 (1993)
- ⁷⁾ Y. Okabe, T. Miwa, A. Takahashi, S. Numata, *Kobunshi Ronbunshu* **50**, 947 (1993)
- ⁸⁾ T. M. Moy, C. D. DePorter, J. E. McGrath, *Polymer* **34**, 819 (1993)
- ⁹⁾ R. Yokota, R. Horiuchi, M. Kochi, H. Soma, I. Mita, *J. Polym. Sci.: Part C: Polym. Lett.* **26**, 215 (1988)
- ¹⁰⁾ M. Ree, D. Y. Yoon, W. Volksen, *J. Polym. Sci., Part B: Polym. Phys.* **29**, 1203 (1991)
- ¹¹⁾ S. Rojstaczer, M. Ree, D. Y. Yoon, W. Volksen, *J. Polym. Sci., Part B: Polym. Phys.* **30**, 133 (1992)
- ¹²⁾ M. Hasegawa, I. Mita, M. Kochi, R. Yokota, *J. Polym. Sci., Part C: Polym. Lett.* **27**, 263 (1989)
- ¹³⁾ M. Hasegawa, H. Arai, I. Mita, R. Yokota, *Polym. J.* **22**, 875 (1990)
- ¹⁴⁾ M. Hasegawa, M. Kochi, I. Mita, R. Yokota, *Eur. Polym. J.* **25**, 349 (1989)
- ¹⁵⁾ E. D. Wachsman, C. W. Frank, *Polymer* **29**, 1191 (1988)
- ¹⁶⁾ U. Goeschel, H. Lee, D. Y. Yoon, R. L. Siemens, B. A. Smith, W. Volksen, *Colloid Polym. Sci.* **272**, 1388 (1994)
- ¹⁷⁾ "Polyimides: Trends in Materials and Applications", C. Feger, M. M. Khojasteh, S. E. Molis, Eds., Soc. Plast. Eng., Mid-Hudson Section, Hopewell Jct., New York 1996
- ¹⁸⁾ T. Miwa, Y. Okabe, M. Ishida, *Polymer* **38**, 4945 (1997)
- ¹⁹⁾ M. Ree, T. L. Nunes, K. J. R. Chen, *J. Polym. Sci., Part B: Polym. Phys.* **33**, 453 (1995)
- ²⁰⁾ M. Hasegawa, Y. Shindo, T. Sugimura, S. Ohshima, K. Horie, M. Kochi, R. Yokota, I. Mita, *J. Polym. Sci., Part B: Polym. Phys.* **31**, 1617 (1993)
- ²¹⁾ M. Hasegawa, J. Ishii, T. Matano, Y. Shindo, T. Sugimura, T. Miwa, M. Ishida, Y. Okabe, A. Takahashi, *ACS Symp. Ser.* **614**, 395 (1995)